

Equilibrium and Kinetic Studies on the Reversible Dissociation of Yeast Enolase by Neutral Salts*

Thomas H. Gawronski† and E. W. Westhead

ABSTRACT: The dissociation of yeast enolase by KCl has been confirmed by the preparation of hybrids of native and acetylated enzyme and by sedimentation equilibrium and gel filtration studies. Examination of the equilibrium between inactive monomers and native enzyme at different concentrations of protein, salt, and magnesium ion show that the equilibrium we observe is a monomer-dimer equilibrium and that the effect of chloride or bromide ion fits a mass action law over the observable range of the equilibrium.

The greater dissociating power of bromide is attributable to a greater number of binding sites for bromide. Acetate is shown to have no measurable dissociating effect while perchlorate and nitrate have effects stronger than bromide or iodide. The effect of magnesium on the equilibrium is not

It has been shown by Brewer and Weber (1966) that high concentrations of KCl reversibly inhibit yeast enolase, and that this inactivation is associated with a reversible dissociation of the molecule into halves (Brewer and Weber, 1968). The present paper is, in effect, in three parts. The first part confirms the reversible dissociation of the enzyme by preparation of hybrids between labeled and unlabeled molecules, and by gel filtration chromatography. The second part deals with the nature of the over-all equilibrium; the response of the system to changes of concentration of protein, salt, Mg^{2+} , and substrate are described. The final part is a study of the rates of dissociation and association over the accessible temperature range.

Materials

Enolase was prepared from Baker's yeast as described elsewhere (Westhead and McLain, 1964). A single chromatographic component, enolase A, was isolated from the purified enolase by chromatography on DEAE-cellulose. This material was used in all the experiments reported here.

* From the Department of Biochemistry, University of Massachusetts, Amherst, Massachusetts 01002. Received April 10, 1969. This work was supported by Grant No. GM14945 from the National Institutes of Health, Department of Health, Education, and Welfare. The work is taken in part from a thesis by T. H. G. submitted to the Molecular Biology Faculty, Dartmouth Medical School, in partial fulfillment of the requirements for the Ph.D. degree. Some of these results have already been presented (*Fed. Proc.* 27, Abstr. 1714 (1968)).

† Supported by Training Grant No. 5-TL-GM-961, awarded to the Molecular Biology Program of Dartmouth Medical School by the National Institutes of Health, Department of Health, Education, and Welfare. Present address: Department of Biochemistry, University of Minnesota Medical School, Minneapolis, Minn. 55455.

readily fitted to a simple model, although it pulls the equilibrium strongly toward active dimer formation. Substrate promotes association, but again the effects are not easily interpreted. The dissociation reaction was found to be first order in protein, and Arrhenius plots are shown for dissociation at different salt concentrations at different magnesium and substrate concentrations. The data indicate that the rate of dissociation is unaffected by the ionic environment. Association reactions are found to be second order initially, and activation parameters have been calculated. Temperature effects on dissociation rates, but not association rates, show a large change in heat capacity for the activation process, similar to cited protein denaturation reactions and indicating exposure of hydrophobic residues to solvent in the monomeric state.

All reagents were analytical reagent grade and were used without further purification except that urea solutions were passed through a mixed-bed ion-exchange column just prior to use. [$1-^{14}C$] Acetic anhydride (10^4 dps/mg) was obtained from New England Nuclear Corp.

Methods

All pH values reported were determined using a Radiometer Model 22 pH-meter.

Conductivity measurements were made at room temperature, using a Radiometer conductivity meter, type CDM-2d.

Optical rotation data in the visible region of the spectrum were obtained with a Rudolph polarimeter. Solutions were passed through a Millipore filter prior to optical rotation measurements to remove particulate matter. Data from concentrated salt solutions were corrected for changes in refractive index (Schellman, 1958).

The extent of acetylation of acyl-enolase and hybrid enolase was determined by scintillation counting of incorporated radioactivity using a refrigerated Packard TriCarb scintillation counter. Aliquots of protein solution were dried on filter paper disks (Whatman 41, 2.5 cm). The disks were placed in counting vials containing 10 ml of a toluene solution of 3.82 g of POPOP¹ and 0.378 g of PPO per l. of solution.

Ultracentrifugation was done with a Spinco Model E ultracentrifuge, using scanning optics at 280 $m\mu$. Scanner data were converted into actual absorbancies by comparing the initial recorded absorbancies (before sedimentation was

¹ Abbreviations used are: POPOP, 1,4-bis[2-(5-phenyloxazolyl)]benzene; PPO, 2,5-diphenyloxazole; PGA, phosphoglycic acid; PEP, phosphoenolpyruvate; BSA, bovine serum albumin.

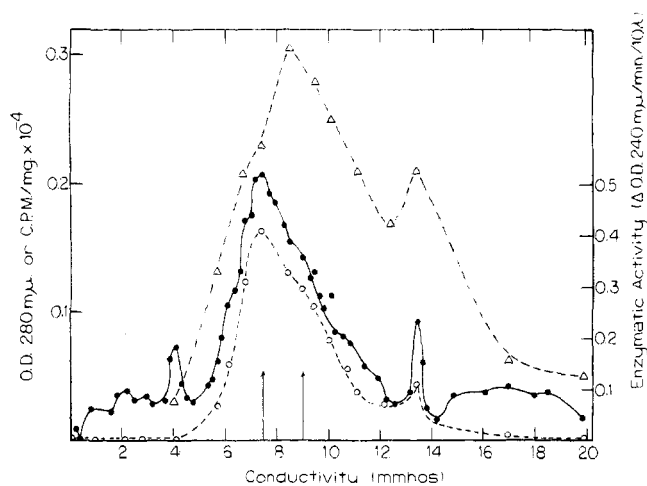


FIGURE 1: Ion-exchange chromatography of partially acetylated enolase A. (●) OD_{280} , (Δ) specific radioactivity, and (○) enzymatic activity. Arrows indicate the portion selected for rechromatography. The elution buffer contained: 1×10^{-3} M $Mg(Ac)_2$, 3×10^{-3} M Tris-Ac, and variable KAc, pH 8.0. Enzyme activity was measured in the standard assay system. Chromatography was at room temperature.

discernible) with the known absorbancies of the solutions, and by correcting for nonlinearity of the scanner with the built-in calibration standards.

Sedimentation equilibria were determined using either Yphantis six-channel cells or double-sector cells. Corrections for the difference in density between salt solutions and water were made for all data. The specific volume of the protein was taken as 0.735 ml/g as given by Bergold (1946).

Sedimentation velocity measurements were made in single-sector cells without reference, using scanning optics. Corrections were made for viscosity and density of the solvent.

Enolase activity was measured at 30° in a solution containing Tris-acetate buffer (pH 7.4), 0.050 ionic strength, 1.0×10^{-3} M magnesium acetate, 2.4×10^{-3} M DL-2-phosphoglyceric acid, and 1×10^{-5} M EDTA. The increased absorbance at 240 or 230 $m\mu$ due to phosphoenolpyruvate formation was followed with a Gilford recording spectrophotometer.

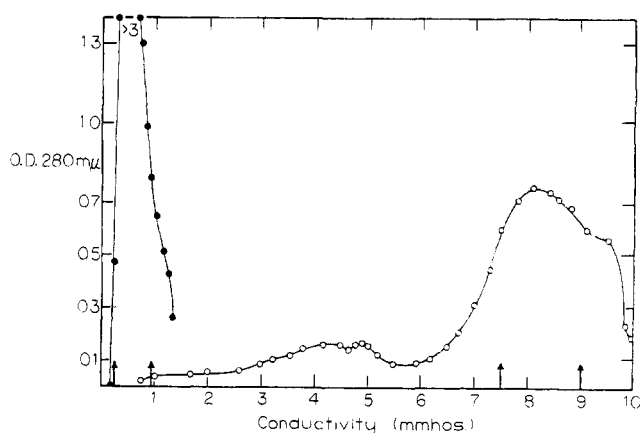


FIGURE 2: Ion-exchange chromatography of enolase A and previously fractionated acyl-enzyme. The data presented are taken from two separate elutions. (●) Native enolase A and (○) acyl-enolase. Elution conditions as in Figure 1.

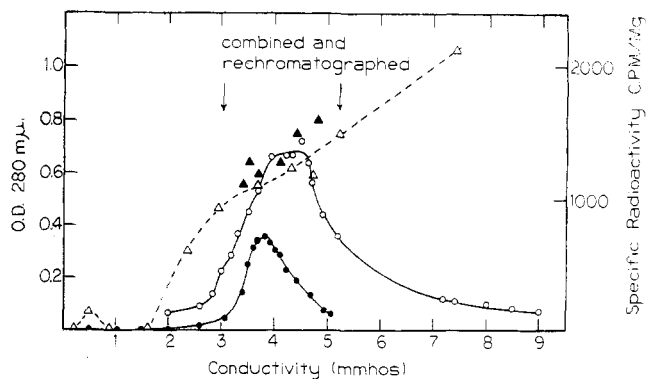


FIGURE 3: Ion-exchange chromatography of enolase hybrids on DEAE-cellulose. Open symbols indicate the original elution results. The arrows indicate the portion which was rechromatographed. The filled symbols indicate the results of the second fractionation. (○) OD_{280} and (Δ) specific radioactivity. Elution conditions as in Figure 1.

Protein concentrations were measured only as the absorbance of the solution at 280 $m\mu$. For pure enolase, 1 mg/ml has an absorbance of 0.89 at 280 $m\mu$ (Warburg and Christian, 1942).

Results

Purification of Enolase A. Pure yeast enolase has been shown to contain several electrophoretic species (Malmstrom, 1957). These species may be resolved using ion-exchange column techniques (Westhead and McLain, 1964). Enolase A, the species with lowest net negative charge and the species eluted from DEAE-cellulose at lowest salt concentration at pH 8.0, was selected for use in these experiments.

The pure enzyme was adsorbed onto a column of DEAE-cellulose at low ionic strength and eluted with stepwise increments in salt concentration. Enolase A is eluted with buffer which has a conductivity of 1 mmho. Eluting buffers contained 10^{-3} M Tris-acetate, 10^{-4} M EDTA, 10^{-3} M magnesium acetate, and sufficient potassium acetate to make the desired conductivity.

The purified enolase A was rechromatographed on DEAE-cellulose. The enzyme was eluted with over 90% of its activity in a single peak emerging between 0.4 and 0.7 μ mho.

Acetylation. Pure enolase A was dialyzed *vs.* 0.1 M potassium borate buffer (pH 9) which also contained: 0.2 M KAc, 2×10^{-3} M $MgAc$, and 10^{-3} M EDTA; 40 moles of $[1-^{14}C]$ -acetic anhydride (10^4 dps/mg) per mole of protein was added at 0° and the solution was stirred for 1 hr. The product was dialyzed *vs.* buffer containing: 0.01 M Tris-Ac, 0.002 M $MgAc$, 0.001 M KEDTA, and 0.04 M KAc (pH 8.0) and chromatographed as described above. The acetylated enzyme proved to be heterogeneous as shown in Figure 1, so the material contained in the indicated tubes was combined, dialyzed, and rechromatographed. The rechromatographed material contained in the indicated tubes shown in Figure 2 was combined. The specific activity of this material was 220 compared with the specific activity of the starting material which was 270.

Preparation and Characterization of Hybrids. Enolase hybrids were prepared from enolase A and the chromato-

TABLE I: Hybridization of Yeast Enolase.

| Sample | OD _{280 mμ} Units | Elution Conductivity (mmho) | cpm/ OD _{280 mμ} |
|-------------------|-------------------------------|-----------------------------------|------------------------------|
| Acyl-enzyme | 51 | 7.5-9.0 | 2870 |
| Native | 156 | 0.5-1.0 | 0 |
| Hybrid | 36.8 | 3.0-5.2 | 1470 |
| Rechromatographed | 35.0 | 3.4-4.8 | 1260 |

graphically purified acyl-enolase by mixing the two in a ratio of approximately 3:1 to maximize hybrid yield from the acetylated enzyme. The solution was made 1 M in KBr by adding solid salt and EDTA was added to a concentration of 0.01 M. The solution was gently stirred for 3 hr, dialyzed *vs.* 10^{-3} M Tris-Ac (pH 8.0)- 10^{-3} M MgAc₂, and chromatographed on DEAE-cellulose. The results are shown in Figure 3. The hybrid peak was dialyzed and rechromatographed. The properties of native, acetyl, and hybrid enzymes are compared in Table I.

The specific enzymatic activity of the rechromatographed fraction was intermediate between that of native and acetyl-enzymes.

The requirement for KBr was shown by allowing a portion of the mixed acyl- and native enzyme to stand without added KBr for 1 hr at pH 8.0 in 0.001 M Tris-acetate buffer containing 10^{-5} M EDTA and 10^{-3} M magnesium acetate. Chromatography of this mixture under the conditions demonstrating hybrid formation, above, showed clean resolution of the mixture into its radioactive and nonradioactive components with no evidence of hybrids.

Molecular Weight Determinations. The existence of hybrids alone does not demonstrate subunit formation since hybrid molecules could also be formed by aggregation of native (67,000 molecular weight) units. Sedimentation equilibrium molecular weight determinations on the hybrid material, however, showed unequivocally that they were subunit hybrids. Sedimentation equilibrium molecular weights at concentrations of 0.6, 0.4, and 0.2 mg per ml extrapolated linearly on a $1/M$ *vs.* C plot to a molecular weight of 57,000. Repeated equilibrium sedimentation experiments at different concentrations of protein, salt, and EDTA consistently showed the dissociating effect of KBr and KCl contrasted with the lack of such an effect by potassium acetate. Representative results are shown in Figure 4. The upper curve, at low protein concentration, showed a uniform molecular weight of 34,000 throughout the entire cell. The lower curve shows that at ten times higher protein concentration, both monomer and dimer are present even in the absence of divalent cations. The lines drawn through the data points have slopes corresponding to molecular weights of 34,000 and 67,000. Brewer and Weber (1968) have shown similar differences between KCl and potassium acetate solutions of the enzyme.

Gel Filtration of Enolase A in Concentrated Salt Solutions. Additional evidence to rule out possibilities of artifact is presented in Figure 5, which shows the results of gel filtration in columns of Sephadex G-150. Dissociated enolase should

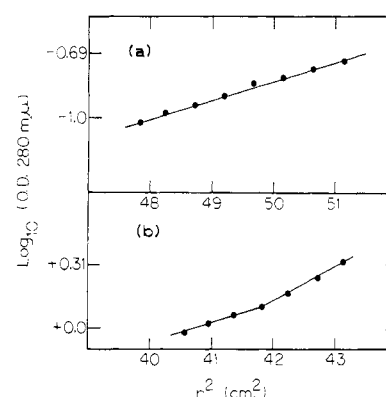


FIGURE 4: Sedimentation equilibrium data plotted for molecular weight determination. Temperature 20°, speed 12,000 rpm. Enzyme dialyzed *vs.* 1 M KBr and 5×10^{-3} M Tris-Ac (pH 8.0). Upper curve: initial protein concentration = 0.160 mg/ml. Lower curve: initial protein concentration = 1.40 mg/ml.

show increased retention in gel filtration. No conformational change in the intact molecule should produce increased retention since it has been shown to be tightly coiled in the native state (Westhead, 1964; Bergold, 1946), and any expansion of the molecule would produce decreased retention. The elution pattern of enolase A was investigated in molar solutions of KAc, KCl, and KBr, all containing 0.01 M EDTA and 0.005 M Tris-Ac (pH 8.0). The BSA is eluted similarly in all solvents while Cl⁻ and Br⁻ both displace the enolase peak to larger elution volumes. In the experiments shown, BSA was used as a marker to detect possible effects of salt on the gel structure. Earlier data, obtained without a marker, showed similar effects of ions on the enolase elution volume.

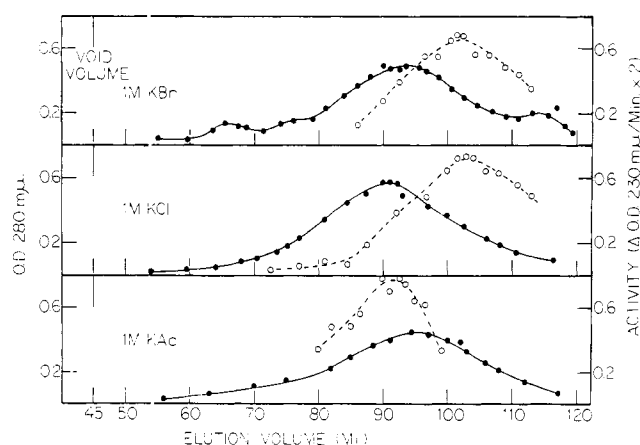


FIGURE 5: Gel filtration of enolase A in several different salt solutions with BSA as marker. Enolase A was chromatographed at room temperature, on a G-150 Sephadex column (2.5×42.7 cm) in the presence of 0.005 M Tris-Ac, 0.01 M EDTA, and 1 M concentrations of either KAc, KCl, or KBr (pH 8.0). The 3-ml sample contained approximately 20 mg of BSA and 0.96 mg of enolase A. Results in KBr, KCl, and KAc are shown in the upper, middle, and lower frames, respectively. (●) Eluate absorbance at 280 mμ. (○) Enolase activity of 10 μl of eluate in 1 ml of assay solution; the aliquots were preincubated in the assay buffer before assay, and optical density changes were monitored at 230 mμ.

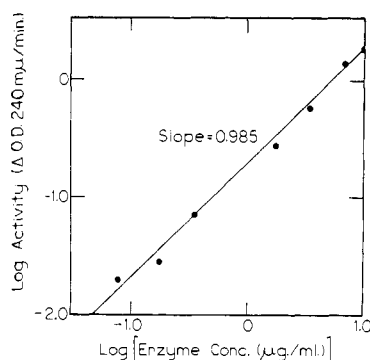
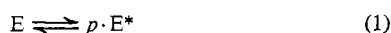


FIGURE 6: Enzyme activity *vs.* protein concentration in the presence of 0.5 M potassium acetate. The standard assay system (at 30°) was used except for the presence of 0.5 M KAc.

Equilibrium Studies

The dissociation equilibrium was found to be influenced by protein concentration, salt concentration, Mg^{2+} concentration, and under some conditions, by substrate concentration. At high salt, low Mg^{2+} , and low protein concentration it is readily established that there is no appreciable active enzyme species present. It is also found that within the time span of the experiments to be described, there is a true equilibrium that may be reached from either direction.

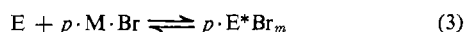
The experiments in this section are designed to test a model based on stoichiometric binding of the effectors, and to determine the stoichiometry of the binding. We use the symbols E , E^* , and E_t for concentrations of native enzyme (active), dissociated subunits (inactive), and total enzyme, respectively. The protein equilibrium alone would thus be



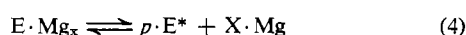
and

$$E_t = E + E^*/p \quad (2)$$

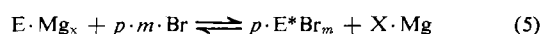
where p is the number of subunits into which the protein dissociates. Since halide ions increase the dissociation, a stoichiometric model would include the binding of, *e.g.*, bromide ion to the subunits, thus



Here $p \cdot M \cdot Br$ is the bromide concentration, and $E^* Br_m$ is the complex between subunits and m ions of bromide. Finally we describe the effect of Mg^{2+} in promoting association by proposing a complex between the native enzyme and Mg^{2+} ion, thus



The complete equilibrium would then have the form



In the following experiments, E_t and E were measured as activity units, since the catalytic activity of the native enzyme varies with the environment. E_t was determined by measuring the initial velocity of the enzyme reaction on addition of

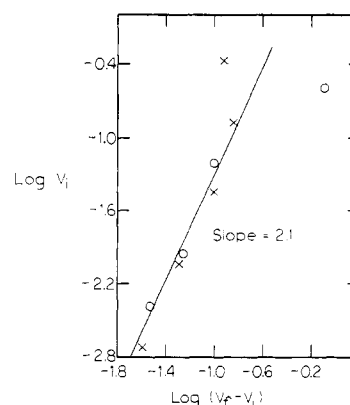


FIGURE 7: Effect of protein concentration on activity in 0.5 M potassium bromide, plotted according to eq 7. Enzyme equilibrated at 30° in the standard assay solution with added 0.5 M KBr. Protein concentrations represented are from 10.6 to 0.035 μ g per ml. Different symbols show two replicate experiments.

native enzyme to the dissociating solvent plus substrate or by extrapolating activities obtained at high protein concentrations where the equilibrium is strongly in favor of association. E was measured as the initial velocity of the reaction upon addition of substrate to a preequilibrated enzyme solution. Attainment of equilibrium took up to 30 min and was ascertained by the constancy of initial velocities in samples with different incubation times. All equilibrium measurements were at 30°, in 1-ml solutions containing Tris-acetate buffer (pH 7.4), 0.05 ionic strength. Other components of the solution are given below and in figure legends. Initial velocities were determined by adding 10 μ l of 0.12 M D-2-PGA to the 1 ml of solution.

Effect of Protein Concentration on Activity of Enolase A in Concentrated Salt Solutions. When enolase A was preincubated in the solution described above, but containing 0.5 M potassium acetate and 10^{-3} M magnesium acetate, no change in catalytic activity occurred with time, and as shown in Figure 6, the activity was proportional to enzyme concentration. In 0.5 M KBr plus 10^{-3} M magnesium acetate, on the other hand, initial enzyme activity at low protein concentrations decreased markedly with time, reaching a limiting value which depended upon the protein concentration. Upon addition of substrate to such a solution a time-dependent increase in catalytic activity was observed. At higher protein concentrations, activity was proportional to enzyme concentration and no increase in activity was seen during the assay.

Referring to the equations and equilibria above we see that an equilibrium constant for reaction 1 can be written as $K = (E^*)^p/E$. Substituting from reaction 2 this becomes

$$K = \frac{(E_t - E)^p (P)^p}{E} \quad (6)$$

Because the concentration of effectors (Mg^{2+} , KBr) is large compared with the enzyme concentration, we can use this simple form of the over-all equilibrium at fixed concentrations of the other effectors. The logarithmic form of reaction 5 appears as

$$\log E = p \log (E_t - E) + p \log (P) - \log K \quad (7)$$

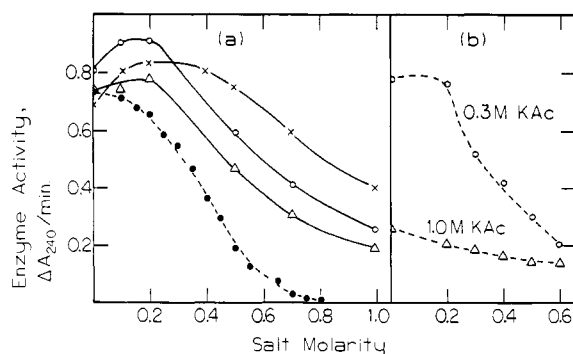


FIGURE 8: Effect of salt concentration on equilibrium activity of enolase. Enzyme was preequilibrated at 30° in the standard assay solution plus indicated salt. Solid lines show effect of KAc; dashed lines, effect of KBr. (a) X, $(\text{Mg}^{2+}) = 2 \times 10^{-3} \text{ M}$; O, $(\text{Mg}^{2+}) = 1 \times 10^{-3} \text{ M}$; Δ , $(\text{Mg}^{2+}) = 5 \times 10^{-4} \text{ M}$. Dashed line in part a shows same data as in Figure 9, but with the ordinate scale normalized for comparison with the acetate data. (b) Effects of KBr on activity in presence of indicated concentrations of KAc.

If this model is valid then, a plot of \log (fractional activity) *vs.* \log (fractional inactivity) determined at various total enzyme concentrations will be a straight line with slope equal to the number of subunits. The actual results are shown in Figure 7. It is seen that the model fits the data over a nearly 30-fold range of protein concentration.

Effect of Salt Concentration on Activity of Enolase A. Enolase A was preincubated as described above, but with the addition of 10^{-3} M magnesium acetate, 10^{-4} M EDTA, and various concentrations of KCl, KBr, or potassium acetate. After allowing equilibrium to be established, the preincubation mixtures were assayed by addition of substrate. Typical results are shown in Figure 8a (dashed curve).

The inhibition by Cl^- or Br^- was sigmoid in character, indicating that the bromide and chloride effects are higher than first order. In the preceding experiments (Figure 7) the coefficient, p , was established as having a value of 2. With this identity an equilibrium equation from reaction 3 can be written as

$$K = \frac{(E^* \text{Br}_m)^2}{(E)(\text{Br})^{2m}} \quad (8)$$

We know that in the absence of KBr or KCl under the conditions used, there is no detectable dissociation so that the total enzyme concentration can be written as $E_t = E + E^*(\text{Br}_m)/2$. Substituting from this into eq 6, and putting the result into logarithmic form we get

$$\log \left[\frac{(E_t - E)^2}{E} \right] = \log K + 2m \log (\text{Br}) - \log 4 \quad (9)$$

A plot of \log (inactive fraction)²/active *vs.* \log (Br) will then be a straight line with a slope of $2m$ if the stoichiometric model fits the data.

This is similar in form to the so-called Hill equation (see, for example, Atkinson, 1966). In the Hill formulation, however, only a conformational transition is predicated while here we are dealing with a dissociation and get a squared term. The data are plotted according to this formulation in

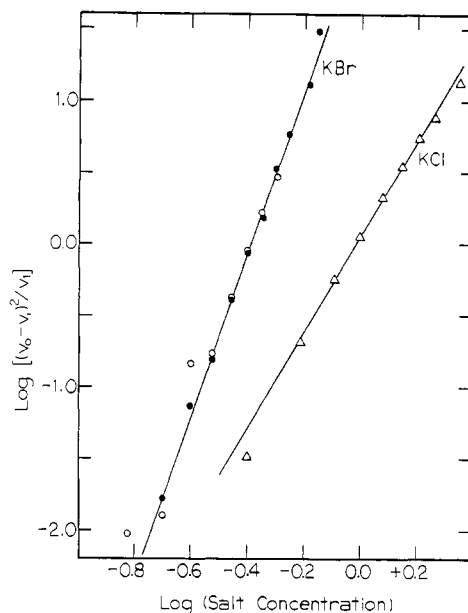


FIGURE 9: Effects of salt concentration on activity plotted according to eq 9. Enzyme was preincubated as in Figure 8. (●) KBr, protein concentration $5.5 \mu\text{g/ml}$; (○) KBr, protein concentration $1.38 \mu\text{g/ml}$; (Δ) KCl, protein concentration $2.39 \mu\text{g/ml}$. Total range of activity represented is about 70-fold.

Figure 9. The slopes of these lines indicate that at least six bromide ions or three chloride ions per native enolase molecule are involved in the dissociation.

Potassium acetate is also an effective enolase inhibitor when present in high concentration. As shown in Figure 6, however, acetate does not produce dissociation. The inhibition by acetate is complex; Figure 8a shows that there is an initial activation by acetate followed by a sigmoid inhibition. This curve cannot be fit to the model used for bromide or chloride inhibition. When acetate is added to preincubation mixtures containing bromide, acetate protects against inactivation. The protection is maximal at 0.3–0.4 M potassium acetate. The data of Figure 8b show typical results when bromide inhibition is examined in the presence of acetate.

Preliminary results with other salts showed inhibition by the potassium salts of ClO_4^- , NO_3^- , SCN^- , and I^- , with half-inhibition of the enzyme at concentrations of 90, 50, 15, and 0.5 mM, respectively. The cation also has a significant effect on the inhibition phenomenon. For example, with an enzyme concentration of 1.3 mg/ml, 0.5 M KBr caused 83% inhibition while 0.5 M tetramethylammonium bromide caused only 45% inhibition. At the same protein concentration, potassium, ammonium, and sodium acetate at 1 M concentration produced 64, 85, and 92% inactivation. In all cases, inactivation is completely reversible unless the enzyme is left for long periods (several hours) in the inactivating salt solution. A slow irreversible denaturation appears to follow the initial dissociation.

Protection by Activating Metal Ions and Substrate. Brewer and Weber (1968) have shown that magnesium ion is effective in protecting enolase against dissociation by chloride ion. We have examined this further in equilibrium systems as described above. Metal ion was removed from the protein by dialysis for several days against 0.1 M EDTA solutions

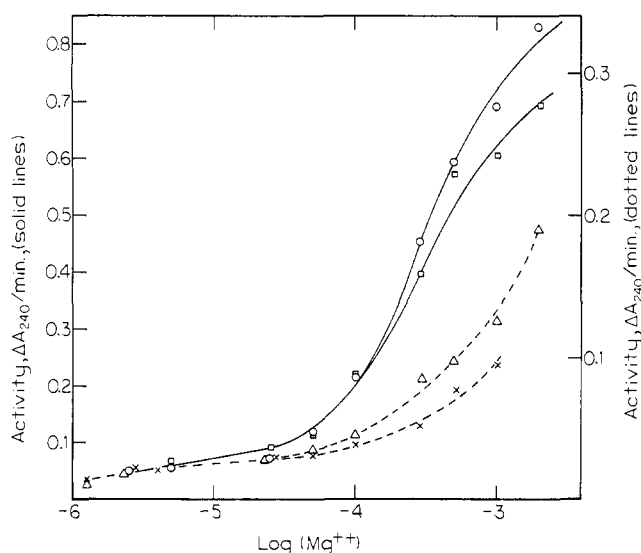


FIGURE 10: Variation of activity with Mg^{2+} and substrate concentration at equilibrium in 0.5 M KBr. Temperature 30° , Tris-Ac buffer, 0.05 ionic strength, pH 7.4. Protein concentration $1.9 \mu\text{g/ml}$ for dotted curves, $3.8 \mu\text{g/ml}$ for solid curves. (○ and Δ) Substrate = 2×10^{-4} M; (□ and ×) no substrate.

and the EDTA was removed by further dialysis. This protein was then diluted more than 1:100 into preincubation mixtures at 30° containing 0.5 M KBr, 0.05 ionic strength, Tris-acetate buffer (pH 7.4), and different concentrations of metal ions. After equilibrium was attained, the initial enzyme activity was determined upon addition of substrate. Where necessary, sufficient Mg^{2+} was added with the PGA to raise the Mg^{2+} concentration to 1×10^{-3} M; 10^{-3} M Mg^{2+} was also used when assaying solutions containing Mn^{2+} . The results of these experiments are shown in Figure 10. These data are not fitted to a theoretical model like the preceding data on protein and salt concentration effects because they do not, in general, form linear plots when so treated. This will be considered in more detail in the Discussion. It will be seen that in two sets of data shown, substrate at 2×10^{-4} M was included in the preincubation solutions. A protective effect of substrate is seen at higher metal ion concentrations. To examine this effect further, preincubation mixtures were prepared with different substrate concentrations and magnesium concentrations of 0 or 10^{-3} M. These equilibrium systems were then assayed by determining the initial velocity of the catalytic reaction when sufficient substrate and magnesium ion was added to bring the concentration of both to the level of the standard assay solution. Suitable controls were run to correct for product inhibition where appropriate.

When Mg^{2+} was not present during preincubation, there was no significant effect of substrate on the level of active enzyme. At concentrations of magnesium around 10^{-4} M, sufficient to cause a definite shift in the equilibrium, there is still little or no effect of substrate addition. At magnesium concentrations an order of magnitude higher, however, the effect of substrate is quite marked as shown in Figures 10 and 11. (It should be noted in passing that "substrate" under conditions of the experiment is an equilibrium mixture of phosphoglyceric acid and phosphopyruvic acid.)

Figure 11 requires explanation; the ordinate is observed

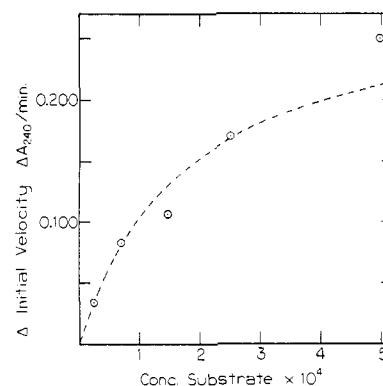


FIGURE 11: The protective effect of substrate. Preincubation mixtures contained normal assay concentrations of Mg^{2+} and buffer at 30° . The preincubation mixtures also contained 0.5 M KBr and the indicated substrate concentration. The protein concentration was $5.9 \mu\text{g/ml}$. The dashed line is a calculated saturation curve with $K_m = 1.8 \times 10^{-4}$ and $V_{\max} = 0.280$. See text (eq 10) for significance of ordinate.

initial activity *minus* the initial activity seen when substrate was not included in the equilibration solution. The justification of this procedure follows.

The equilibrium mixture contains active enzyme, inactive subunits, and the enzyme-substrate complex. Under conditions where the enzyme would be fully associated if KBr were absent and fully dissociated if Mg^{2+} were absent, we can write $E_t = E + E^* + ES$, where E now represents EMg_x and E^* represents E^*Br_m . At equilibrium, $E^* = K(E)$ and $ES = (E)(S)/K_s$. Our initial velocity on addition of excess substrate measures $E + ES$. With the usual kinetic derivation procedures, it can be shown that

$$ES = \frac{E_t}{1 + \frac{K_s}{S}(1 + K)}$$

Since

$$E = (ES) \frac{K_s}{(S)}$$

the sum of ES and E is

$$(ES + E) = \left(1 + \frac{K_s}{S}\right) \frac{E_t}{1 + \frac{K_s}{S}(1 + K)}$$

When the substrate concentration in the equilibrium mixture approaches zero, K_s/S is much greater than one, so

$$(ES + E)_{S \rightarrow 0} = \frac{E_t}{1 + K}$$

By subtracting this value from the initial velocities observed when substrate is present in the equilibrium mixture, we get

$$(ES + E) - (ES + E)_{S \rightarrow 0} = E_t \left[\frac{K/(1 + K)}{1 + \frac{K_s(1 + K)}{S}} \right] \quad (10)$$

which obviously has the form of a rectangular hyperbola. At low values of K , the Michaelis-Menten expression appears.

At more significant values of K , the half-maximum constant for the hyperbolic function becomes a combination of the substrate binding constant and the protein equilibrium constant. These apparent constants are of course actually functions of the KBr and Mg^{2+} concentration. At lower concentrations of Mg^{2+} , K would be large, and the half-maximum constant for the substrate effect would increase to levels impractical to reach with our experimental design. At higher concentrations of Mg^{2+} , K is decreased toward the actual value of K_s . From the data of Figure 11, one can make a plot of $(\Delta \text{ initial velocity})^{-1}$ vs. (substrate concentration) $^{-1}$ and get a good straight line fitting a constant of 1.8×10^{-4} , which is within a factor of 2 of the values for K_m for the native enzyme under these conditions.

Kinetic Studies

Rates of Inactivation. In our equilibrium studies of enolase inactivation, we found that bromide-produced inactivation required several minutes under some conditions. We hoped that the kinetics of inactivation would yield some information about the nature of the process.

The measurements were made by putting the enzyme into the assay cuvet containing a specified concentration of potassium bromide, 0.5, 0.75, or 1.0 M, as well as the usual assay concentrations of Tris-Ac, magnesium acetate, and EDTA. In some experiments, the cuvet also contained 2.0×10^{-4} M DL-2-PGA. After preincubation for a measured time, the reaction was initiated by addition of substrate to the usual assay concentration and the initial velocity was measured. The zero-time enzyme activity was measured by adding the native enzyme directly to a cuvet containing all the usual components of the assay mixture plus potassium bromide and measuring the initial velocity. When plotted as first-order reactions, the data for inactivation fit a straight line for more than 75% of the reaction. Data taken at various temperatures were used to construct the Arrhenius plots shown in Figure 12. The marked curvature of these plots is well beyond experimental error, and may reasonably be ascribed to an important change in heat capacity for the inactivation process. A smooth curve was drawn through the data as shown, and points were taken from those curves, at places indicated by the three arrows in Figure 12, to calculate thermodynamic parameters from the expression

$$\Delta F^\ddagger = A + BT + CT \ln T \quad (11)$$

By choosing three equally spaced values of T , one can get three equations easily solved simultaneously to give the curve-fitting parameters. Then $\Delta H^\ddagger = A - CT$, $\Delta S^\ddagger = -B - C [\ln T + 1]$, and $\Delta Cp^\ddagger = -C$ (see Brandts, 1964). The values obtained in this way for the four curves shown are the same within experimental error; for ΔH^\ddagger at 25° , the values for the four curves vary between +42 and +47 kcal; the values of ΔS^\ddagger are between +73 and +150 eu at the same temperature and the values of ΔCp^\ddagger are between 1900 and 2400.

Rates of Reassociation. The recovery of enzyme activity, after loss in preincubation mixtures containing 1.0 M KBr and 0.005 M EDTA, was followed by dilution of the enzyme into the complete assay system. Ten microliters or less of enzyme solution was used, reducing the KBr concentration

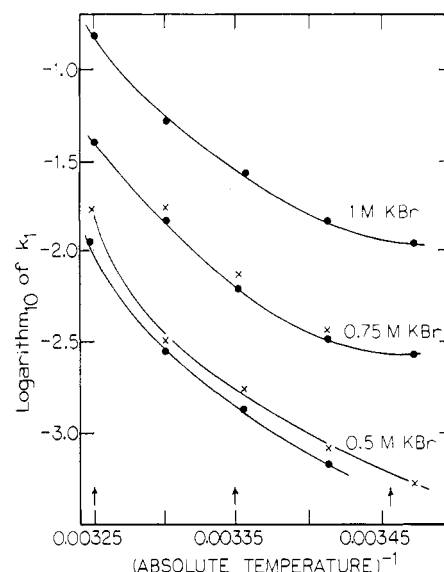
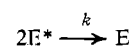


FIGURE 12: Arrhenius plots for dissociation of enolase in presence and absence of substrate at 0.5, 0.75, and 1.0 M KBr. Arrows indicate temperatures at which points on curves were taken to solve eq 11 in text. (●) Data obtained in presence of 2×10^{-4} M substrate and (x) data obtained in absence of substrate. All at pH 7.4 Tris-Ac buffer of 0.05 ionic strength.

to 0.01 M which has no effect on enolase activity. The reaction mixture contained three times the usual concentrations of substrate and magnesium ion and was monitored at 230 μ to extend the linear phase of the reaction. The value for maximal recovery was obtained by preincubation of the enzyme in the assay solution, but without substrate, for 1 hr or more. The reaction was initiated in these control systems by addition of substrate. No further recovery of activity was observed in these assays.

Due to the presence of considerable scatter in the data, attempts, aided by a computer, to fit data from a single recovery curve to an equation for a given kinetic order of reaction gave equivocal results. We then observed the recovery process in a series of enzyme concentrations at several temperatures. The time required for 50% recovery was plotted vs. the reciprocal of maximum enzyme activity and the slope of the lines was determined by a least-squares calculation. The data are shown in Figure 13.

This treatment of the data was chosen because we might imagine that either some first-order configurational change or the second-order recombination of subunits could be rate limiting in the regaining of catalytic activity. In the former case, the half-time, $t_{1/2}$, for recovery of activity would be constant, independent of protein concentration. In the latter case, $t_{1/2}$ will be proportional to the reciprocal of the initial protein concentration. This relationship is easily derived. If



then

$$d(E)/dt = k(E_t - E)^2$$

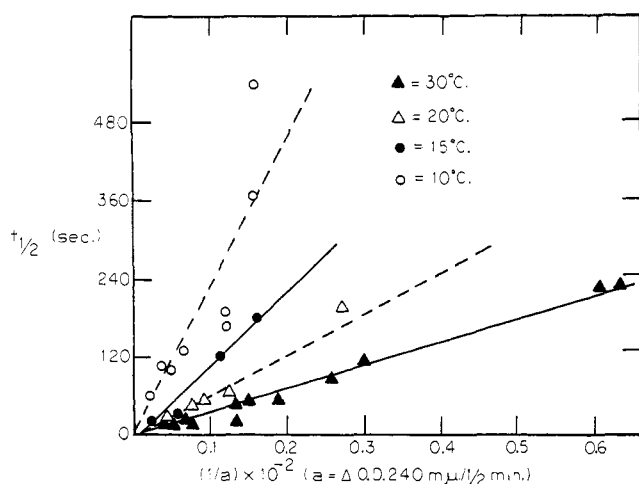


FIGURE 13: Reassociation kinetics of enolase. Enzyme was preincubated at 30° in assay buffer and 1.0 M KBr. Aliquots were diluted 100-fold into assay solution with PGA concentration 7.2×10^{-3} M, Mg^{2+} concentration 3.6×10^{-3} M. ΔA_{280} was recorded. Time for half-recovery is plotted against reciprocal of maximum recovered activity.

and after integration we get $kt = (E_t - E)^{-1}$. At $t_{1/2}$, $E = E_t/2$, so that $kt_{1/2} = (E/2)^{-1}$. It can be seen that data obtained only in the earlier portion of the recovery curve fits a second-order curve quite well. This is in contrast to the attempts to analyze complete recovery curves mentioned above. Figure 14 shows an Arrhenius plot of the data in Figure 13. The thermodynamic parameters calculated from Figure 14 are 11.1 kcal/mole for ΔH^\ddagger and 8.2 eu for ΔS^\ddagger .

Discussion

The apparent production of hybrid enolase was first shown by Brewer and Weber (1968) who labeled enolase with a fluorescent dye and then treated a mixture of the native and labeled protein with 2 M KCl. The formation of hybrids was deduced by the change in depolarization of fluorescence. Our experiments in which the hybrid molecules have been isolated and shown to have the dimeric molecular weight confirm the validity of that interpretation. We hoped that acetylation of the native enzyme might yield differentially reacted subunits if their composition or configuration were different enough. This might have aided in the separation of the two halves of the molecule. Unfortunately, the labeling seems indiscriminate and we did not observe two chromatographically different hybrids.

Numerous molecular weight determinations by the sedimentation equilibrium technique have consistently shown that although magnesium ion helps to cause dimer formation, it is not required. Figure 4b is typical of centrifugation data at higher protein concentrations, showing the presence of native molecular weight material in 1 or 2 M KBr in the absence of divalent metals (in the presence or absence of EDTA). The same phenomenon was described by Brewer and Weber (1968) who showed the presence of both monomer and dimer in KCl solutions containing excess EDTA. The curvature in Figure 4b shows that the equilibrium reaction is slow compared with the transport times in the ultracentrifuge cell (Rao and Kegeles, 1958), and it has been shown

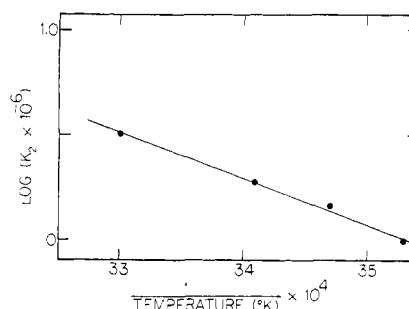


FIGURE 14: Arrhenius plot for reassociation of enolase. Data are taken from slopes of lines in Figure 13.

that reactions with half-times of about 100 sec should fall into this category (Nichol *et al.*, 1964). The lines drawn through the data points in Figure 4b have slopes calculated for the molecular weights of monomer and dimer (34,000 and 67,000). The fit of the data to such a broken line is consistent with the slow equilibration expected from our kinetic data. Data obtained with scanner optics and short columns were judged too imprecise to warrant a more quantitative analysis of these data. The effects of protein concentration, salt concentration, and magnesium ion concentration on the monomer-dimer equilibrium have been interpreted by us according to the model shown in eq 5 above. The effects of protein and salt concentration fit this model very well. The data of Figure 7, for example, test the model over a 250-fold range of equilibrium ratios of monomer to dimer. Those in Figure 9 extend over a 70-fold range. The protein concentration data thus agree completely with the molecular weight determinations.

Of more general importance is the fact that a mass action model accounts so very well for the effect of KCl and KBr. This is a strong argument that the anion effects are caused by direct binding to the protein and not by an environmental effect such as charge shielding or an effect on water structure as postulated for the conformational effects of anions on collagen (Von Hippel and Wong, 1963, 1964). Robinson and Jencks (1965) studied the effects of anions on the solubility of acetyltetraglycine ethyl ester and concluded that their data, too, was best explained by a direct-binding model. In the two references just quoted, and in other recent work (Bezkorovainy, 1966; Nagy and Jencks, 1965; Fridovich, 1963) it is seen that although anion effects seem to occur with a predictable order of effectiveness, the actual behavior is different for different systems. Thus Bezkorovainy (1966) found aggregation of transferrin by several anions (not acetate), and Fridovich (1963) found completely noncooperative inhibition of acetoacetic acid decarboxylase.

In our case, the determination of cooperativity, from the slopes of Figure 9, makes it appear that the greater effectiveness of Br^- over Cl^- is best explained by Br^- binding effectively at *more sites* than does Cl^- . It should be noted that in Figure 9, the slope of the Br^- curve is the same for two protein concentrations even though a higher Br^- concentration is required to dissociate the protein at higher protein concentrations. This again strengthens confidence in the stoichiometric binding model.

It would have been very desirable to do all our work at constant ionic strength. This was not possible because we

could find no truly indifferent electrolyte. We have shown that different anions and cations have different effects on the equilibrium and it is not obvious how we could use one electrolyte in the presence of another without getting competitive effects. It is also clear that acetate, for example, is a fairly effective inhibitor at higher concentrations, without effecting dissociation of the protein. This nondissociative inhibition appears to be insignificant in the case of KBr and KCl because our data, both equilibrium and kinetic, fit a model which does not include inactive dimers.

The data treatment used for protein concentration and salt concentration effects might also have been suitable for the effects of Mg^{2+} concentration. Plots of $\log [(inactive\ enzyme)^p / (active\ enzyme)]$ vs. $\log Mg^{2+}$ would have given straight lines with a slope equal to X , the number of Mg^{2+} ions involved in maintaining the dimeric structure. Such plots were made, but were not linear. We attribute the breakdown of the model at this point to the fact that there are 2 moles of divalent cation bound per mole of native enzyme, and that the two cations are not bound equivalently. This fact has been amply demonstrated in a companion publication (Hanlon and Westhead, 1969). This explanation implies that both of the metal ions bound to the native enzyme significantly effect the strength of the subunit association. It would, of course, be possible to derive an equation for this slightly more complex model, and test its conformity to our data. We believe, however, that the additional parameter would give us sufficient curve-fitting freedom to invalidate any correlation we might make. Too many factors are impractical to weigh; for example, the data shown in Figure 10 are obtained at metal concentrations as low as 10^{-6} M. The KBr was recrystallized from EDTA and then twice from deionized water, but it may be that there were still significant levels of divalent cation (or EDTA) in the KBr. Furthermore, when native enolase is incubated in the absence of metal ion, it undergoes a slow change to an inactive form which is not readily reversed. The extent to which such a change takes place at low metal concentrations in KBr is not easily assessed.

Finally, we know that metal-free dimers exist (Figure 4b). In the experiments at varying protein or salt concentration, the presence of Mg^{2+} rules out the presence of such species. In the metal concentration experiments, however, we may have significant amounts of metal-free dimer.

The effect of substrate on the equilibrium is also difficult to interpret quantitatively. In the present system, substrate was found to give no protection, even at 7×10^{-3} M, when magnesium was at 5×10^{-5} M but protection was readily observable when magnesium was 5×10^{-4} M. Substrate has also been shown to protect the enzyme against iodoacetate (Brake and Wold, 1962) and against photooxidation (Westhead, 1965) only in the presence of metal ions.

These results appear to be in conflict with the fact that, kinetically, substrate and metal bind independently to the enzyme (Hanlon and Westhead, 1969), and that substrate does not interact with the metal ion which appears to be important in promoting association (Hanlon and Westhead, 1969). However in the case of the iodoacetate inactivation it has recently been shown that there is no inactivation except at high concentrations of salt (Westhead and Boerner, 1969). The protection by substrate therefore appears to be due to prevention of salt-induced exposure of sensitive groups.

The fact that substrate does not appear to protect against

dissociation at low Mg^{2+} concentrations does not imply that the divalent metal is required for substrate binding to the native enzyme. The equations developed in the Experimental Section on substrate effects show that *if* substrate is bound independently of Mg^{2+} , but *only to the dimer*, then at low concentrations of dimer, detectable substrate protection will require very high concentrations of substrate. By shifting the equilibrium toward dimer formation, Mg^{2+} can lower the substrate concentration needed to shift the equilibrium in an observable range.

The peculiar features of this enzyme discussed here and in the two preceding papers (Hanlon and Westhead, 1969) tempt one to speculate on possible control sites on the enzyme. However, no effect on the activity has been observed by ATP, ADP, AMP, pyruvate, or fructose diphosphate. There is no good evidence yet on the identity or nonidentity of the two chains. The high salt concentrations required to dissociate it are not suitable for most separation techniques. The fact that the tight binding sites for Mn^{2+} and Mg^{2+} are not the same sites (Hanlon and Westhead, 1969; Figure 5) yet a difference spectrum arises from binding of a metal at either (but not both) sites (Hanlon and Westhead, 1965) suggests the possibility of an anticooperative interaction between two similar sites. The large differences in dissociation constants for the two metal ions bound per mole of native enzyme must indicate either nonidentity of the chains or anticooperative interaction between them.

Negative cooperativity among apparently identical chains has been shown for rabbit muscle glyceraldehyde 3-phosphate dehydrogenase binding of DPN (Conway and Koshland, 1968; DeVijlder and Slater, 1968).

The data in Figures 12 and 14 are not extensive nor of high precision. Nevertheless, the basic implications of the data are sufficiently striking that even a semiquantitative examination of them is worthwhile. Most noteworthy is the curvature of the Arrhenius plots in Figure 12, implying a large change in heat capacity, C_p , between the native dimeric molecule and the transition state on the pathway to dissociation. The contrast between Figure 12 and Figure 14 shows that this large ΔC_p is not matched by a similar ΔC_p between the monomer state and the transition state. The large change in heat capacity indicates a considerable change in the environment of substantial numbers of apolar groups (Brandts, 1969), while the positive sign of ΔC_p indicates that in the dissociation process, apolar regions are exposed to the polar medium. The apparent similarity between the transition state and the monomeric state suggests that these apolar regions remain exposed to the solvent in the dissociated state.

This appears to be the first time that such large heat capacity changes have been observed for a dissociation-association reaction, although very similar ΔC_p 's have been recorded, for the denaturation reactions of ribonuclease (Brandts and Hunt, 1968; Danforth *et al.*, 1967), of trypsinogen (Pohl, 1968), and of chymotrypsinogen (Brandts, 1964). The heat capacity changes and ΔH 's for the ribonuclease thermal transition were found to be 2500 and 88 kcal, respectively, compared with our average values of 2200 and 45 kcal. If the ΔC_p for the transfer of a valyl side chain from the interior of a protein to an aqueous environment is taken as about 50/mole (Brandts, 1969), our average value of 2200 would represent the exposure of about 44 valyl equiv or 22 per

monomer, or about 20% of the hydrophobic residues of the enzyme based on the known amino acid composition (Malmström *et al.*, 1959).

This large-scale exposure of apolar groups to the aqueous environment is surprising in view of our findings that there is no change in the optical rotatory dispersion of the protein. (These results will be reported in detail in a later publication.) This same observation has been made for the denaturation of chymotrypsinogen (Brandts, 1964). Even more striking is our observation (to be reported on later) that not only is the dimer stable in 8 M urea, but that dimerization will readily take place in that medium, despite the fact that the helical structure is substantially disrupted.

Acknowledgment

We thank Mrs. Gema Donahar and Mr. Edward Macloskey for help with some of these experiments and we want to express our appreciation to Dr. John Brandts for valuable discussions about the thermodynamic aspects of this work.

References

- Atkinson, D. E. (1966), *Ann. Rev. Biochem.* 35, 85.
 Bergold, G. (1946), *Z. Naturforsch.* 1, 100.
 Bezkorovainy, A. (1966), *Biochim. Biophys. Acta* 126, 286.
 Brake, J. M., and Wold, F. (1962), *Biochemistry* 1, 386.
 Brandts, J. F. (1964), *J. Am. Chem. Soc.* 86, 4302.
 Brandts, J. F. (1969), in *Protein Structure and Stability*, Timasheff, S., Ed., New York, N. Y., Marcel Dekker.
 Brandts, J. F., and Hunt, L. (1968), *J. Am. Chem. Soc.* 89, 4826.
 Brewer, J. M., and Weber, G. (1966), *J. Biol. Chem.* 241, 2550.
 Brewer, J. M., and Weber, G. (1968), *Proc. Natl. Acad. Sci. U. S.* 59, 216.
 Conway, A., and Koshland, D. E., Jr. (1968), *Biochemistry* 7, 4011.
 Danforth, R. H., Krakauer, H., and Sturtevant, J. (1967), *Rev. Sci. Instr.* 38, 484.
 DeVijlder, J. J. M., and Slater, E. C. (1968), *Biochim. Biophys. Acta* 167, 23.
 Fridovich, I. (1963), *J. Biol. Chem.* 238, 592.
 Hanlon, D. P., and Westhead, E. W. (1965), *Biochim. Biophys. Acta* 96, 537.
 Hanlon, D. P., and Westhead, E. W. (1969), *Biochemistry* 8, 4247, 4255.
 Malmström, B. G. (1957), *Arch. Biochem. Biophys.* 70, 58.
 Malmström, B. G., Kimmel, J. R., and Smith, B. L. (1959), *J. Biol. Chem.* 234, 1108.
 Nagy, B., and Jencks, W. P. (1965), *J. Am. Chem. Soc.* 87, 2480.
 Nichol, L. W., Bethune, J. L., Kegeles, G., and Hess, E. L. (1964), *Protein* 2, 330.
 Pohl, F. M. (1968), *European J. Biochem.* 4, 373.
 Rao, M. S. N., and Kegeles, G. (1958), *J. Am. Chem. Soc.* 80, 5724.
 Robinson, D. R., and Jencks, W. P. (1965), *J. Am. Chem. Soc.* 87, 2470.
 Schellman, J. A. (1958), *Compt. Rend. Trav. Lab. Carlsberg* 30, 363.
 Von Hippel, P. H., and Wong, K. Y. (1963), *Biochemistry* 2, 1387.
 Von Hippel, P. H., and Wong, K. Y. (1964), *Science* 145, 577.
 Warburg, O., and Christian, W. (1942), *Biochem. Z.* 310, 384.
 Westhead, E. W. (1964), *Biochemistry* 3, 1062.
 Westhead, E. W. (1965), *Biochemistry* 4, 2139.
 Westhead, E. W., and Boerner, P. (1969), 157th National Meeting of the American Chemical Society, New York City, N. Y., Sept.
 Westhead, E. W., and McLain, G. (1964), *J. Biol. Chem.* 239, 2464.